# MICROSTRUCTURE AND ELECTRICAL CONDUCTIVITY OF NI/YSZ CERMETS FOR SOFC

**Z.-C. Chen, Y. Sakane, T. Tsurumaki, Y. Ayame and F. Fujita**
**Department of Materials Science and Engineering, Tohoku University, Sendai 980-8579, Japan**

**Keywords**: *SOFC, anode, nickel, YSZ, microstructure, electrical conductivity, porosity*

***Abstract***

*To improve Ni network structure in Ni/YSZ cermet anode, the effect of particle sizes of Ni and YSZ on microstructural evolution, electrical conductivity, and porosity of Ni/YSZ cermets has been investigated. Ni particles with submicron order have been incorporated into YSZ matrix by using nickel nitrate as one of the starting materials. The formation of small-sized Ni particles not only promotes the development of a continuous Ni network in Ni/YSZ cermets and causes improvement in electrical conductivity, but also leads to increase in porosity. When pre-calcined coarse YSZ powder is incorporated into Ni/YSZ cermets, continuous Ni network is easily formed, which contributes to the improvement in electrical conductivity and porosity as well.*

## 1 Introduction

A fuel cell is an energy conversion device that converts the chemical energy of gaseous fuels directly into electric energy via an electrochemical process. Solid oxide fuel cells (SOFCs) have attracted much attention for their high energy conversion efficiency, low emission of pollutants (chemical pollutants and noise), and fuel flexibility [1]. At present, yttria-stabilized zirconia (YSZ) and Ni/YSZ cermet are the most frequently adopted materials for electrolyte and anode, respectively. As an anode, it should have high electrical conductivity, good adherence to other cell components (especially YSZ electrolyte), high electrochemical or catalytic activity, and high porosity to provide diffusion paths for fuel and reaction products [2]. These require the formation of continuous network structures of both Ni and YSZ components, rich three-phase boundary (TPB) sites among Ni, YSZ, and micropores [3,4], and small differences in sintering shrinkage and coefficient of thermal expansion (CTE) between electrolyte and anode. Under essential prerequisite for high electrical conductivity, it is important to decrease Ni amount in Ni/YSZ anode to make the CTE of the anode compatible with YSZ electrolyte.

It has been reported that powder size has a significant effect on microstructure, electrical behavior, and strength of Ni/YSZ anodes [5-8]. The electrical conductivity of a Ni/YSZ cermet depends not only on Ni content in the cermet, but also on morphology, size, and distribution of Ni and YSZ phases. The distribution of Ni particles in a cermet anode has an important effect on the amount of electrode reaction sites (or TPB length) and formation of current path [9].

In order to improve Ni network structure in the cermets and obtain Ni/YSZ cermets with high performance, in the current work, small-sized Ni particles have been incorporated into the cermets by using nickel nitrate as one of the starting materials. Another approach was to incorporate coarse YSZ particles which were obtained by calcining commercial YSZ powder at a high temperature. The objective was to examine the effect of particle sizes of two constituent components, Ni and YSZ, on microstructure, electrical conductivity, and porosity of Ni/YSZ cermets.

## 2 Experimental Procedure

A powder metallurgy route was used to prepare Ni/YSZ cermets with different volume fractions of Ni ($V_{Ni}$=0.2-0.6). As the starting materials, comercially available nickel nitrate ($Ni(NO_3)_2 \cdot 6H_2O$), nickel oxide with two different average particle sizes (1.6μm and 4.7μm, denoted as NiO(S) and NiO(L) respectively), and YSZ (0.54μm (YSZ(S))) powders were used. The as-received YSZ(S) powder was calcined at 1573K for 8h to obtain coarse YSZ powder (YSZ(L)) with an average size of 47.3μm. To adjust particle size distribution and improve the formability, the coarse YSZ(L) powder was mixed

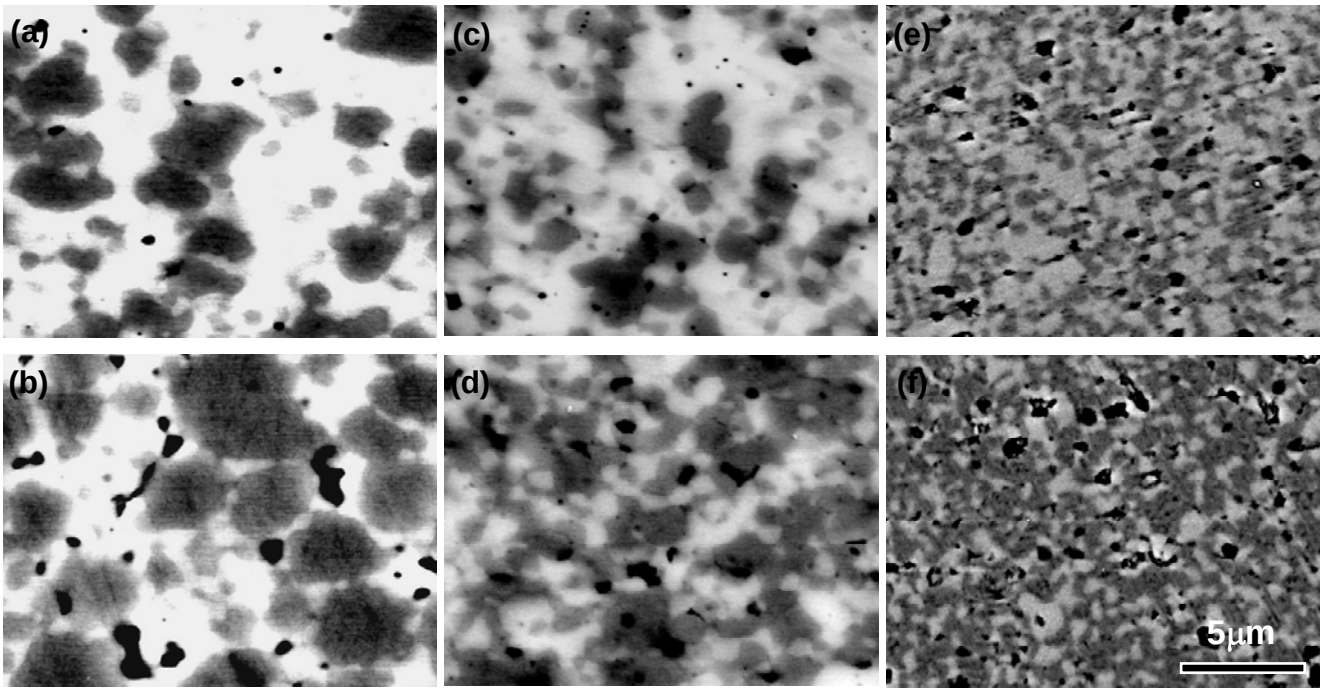


Fig. 1. Microstructures (backscattered electron images) of sintered NiO/YSZ composites, obtained from different powder combinations of (a) (b) NiO(L)/YSZ(S), (c) (d) NiO(S)/YSZ(S), and (e) (f) $Ni(NO_3)_2$/YSZ(S). Upper: $V_{Ni}$ = 0.3 and lower: $V_{Ni}$ = 0.5.

with fine YSZ(S) powder at different mixing ratios. The powders were mixed by ball-milling in ethanol for 24h and then dried. When nickel nitrate was used, the mixed powders were calcined in air at 723K to decompose nickel nitrate into NiO. The resultant powders were consolidated by uniaxially pressing at a pressure of 100-200MPa. The sintering was performed in air at 1673K, followed by reduction in $H_2$ atmosphere at 1273K for 4h.

The crystalline phases in powders, sintered, and reduced samples were identified by X-ray diffraction (XRD) with Cu$K_\alpha$ radiation, and the microstructures were characterized by scanning electron microscopy (SEM). The porosity in sintered and reduced samples was derived by measuring the dimensions and weights of the samples. The electrical resistivity of reduced Ni/YSZ cermets was measured at room temperature using a four-probe method. In addition, the linear shrinkage behavior during sintering was measured by a thermomechanical analysis (TMA) apparatus. Cylindrical specimens were heated in air at a heating rate of 10K $min^{-1}$ to a soak temperature of 1673K and held for 2h.

## 3 Results and Discussion

### 3.1 Effect of Ni Particle Size

XRD analysis showed that the nickel nitrate in $Ni(NO_3)_2$/YSZ powder mixtures was completely decomposed into NiO during calcining at 723K, and the sintered samples had almost the same XRD patterns as those of the calcined powders. Consequently, even though different Ni sources, NiO(L), NiO(S), and $Ni(NO_3)_2$, were used in the experiments, all sintered samples consisted of two phases, NiO and YSZ. Nevertheless, the sizes of NiO particles have a pronounced effect on microstructure of sintered NiO/YSZ composites, in particular, the distribution and morphology of NiO phase within the YSZ matrix.

Fig. 1 shows the microstructures (SEM images in backscattered electron mode) of the sintered NiO/YSZ composites when different Ni sources were used. The light and gray phases in the micrographs correspond to YSZ and NiO, respectively, and the dark regions are pores remaining after sintering. For the sample from NiO(L)/YSZ(S) powder, the NiO was mainly distributed in YSZ matrix as discrete and isolated particles at a volume fraction ($V_{Ni}$) of 0.3 (Fig. 1(a)). Although some particles were connected each other, the degree of connectivity of NiO particles was low. With an increase in $V_{Ni}$, the continuity of NiO particles increased (Fig. 1(b)). When NiO(S) powder

with a smaller average particle size (1.6μm) was used as one of the starting powders, the dispersion and continuity of NiO particles were highly improved (Figs. 1(c) and (d)). At $V_{Ni}$ = 0.5, a continuous NiO network seems to be formed.

In the case of nickel nitrate (Figs. 1(e) and (f)), both NiO and YSZ phases in the micrographs became much finer, compared to the microstructures from larger-sized NiO(L) and NiO(S) powders. The majority of NiO particles were connected together and exhibited a branching cluster structure at $V_{Ni}$ = 0.3. The connection between NiO particles was significantly improved, in comparison with the microstructures with the same Ni content (Figs. 1(a) and (c)). At $V_{Ni}$ = 0.5, a complete NiO network was formed, and it appears that the microstructure is characterized by two interconnecting networks of Ni and YSZ phases. These facts indicate that NiO network is easily formed when nickel nitrate is used as a raw powder. In other words, a continuous NiO network can be achieved at a lower $V_{Ni}$ in the case of nickel nitrate. This is attributed to much smaller sizes of NiO particles, which are formed through decomposition of nickel nitrate during the calcining process.

When NiO/YSZ composites are reduced in $H_2$ atmosphere, NiO is transformed into metallic Ni. Obviously, the sizes of Ni particles in Ni/YSZ cermets strongly depend on those of NiO particles in sintered samples. Microstructural observations showed that the Ni particles had an average size of ~0.3μm. The connection state of Ni particles in resulting Ni/YSZ cermets was evaluated by measuring electrical resistivity of the reduced samples. Fig. 2 illustrates the variation of electrical resistivity of Ni/YSZ cermets as a function of volume fraction of Ni. The electrical resistivity became lower with the decrease in NiO particle size. In particular, the cermets obtained from $Ni(NO_3)_2$/YSZ(S) exhibited the lowest values of electrical resistivity in all cases, showing better electrical conductivity. This is the result of formation of Ni particles with submicron order and thus fine Ni network when $Ni(NO_3)_2$/YSZ(S) powder mixtures are used.

According to the percolation theory [10], inclusions in a random system will form a long-range continuous network, when the volume fraction of the inclusions reaches a critical value (percolation threshold). The percolation threshold has been found to decrease with increasing the ratio of matrix size to inclusion size [11-13]. In the case of NiO/YSZ system examined in the current work, however, in addition to physical touching between neighboring particles like rigid inclusions, the sintering densification takes place in both NiO and YSZ phases, giving rise to further microstructural developments of the second phase. Our previous investigation [14] has examined the microstructural evolution and densification behavior of metal-ceramic composites, where two constituent components, stainless steel and zirconia, were sintered simultaneously. The zirconia phase exhibits a branching cluster structure in a stainless steel matrix (large particle size ratio), while the stainless steel phase is dispersed randomly throughout the zirconia matrix in the form of equiaxed particles (small particle size ratio).

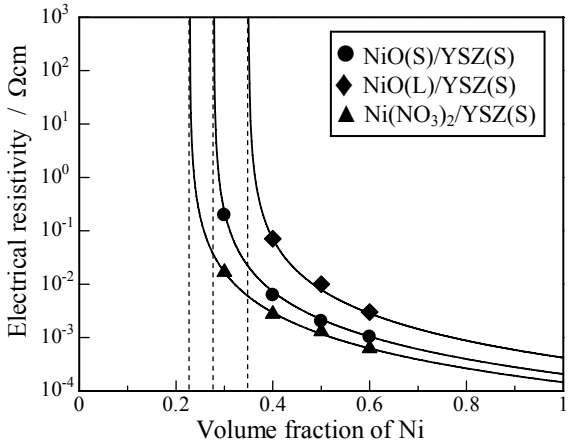


Fig. 2. Variation of electrical resistivity of Ni/YSZ cermets as a function of $V_{Ni}$.

By using the measured data of electrical resistivity, the curves of electrical resistivity versus volume fraction of Ni were drawn in Fig. 2. The percolation threshold values were estimated as $V_{Ni}$ = 0.23, 0.28, and 0.35 for different powder combinations of $Ni(NO_3)_2$/YSZ(S), NiO(S)/YSZ(S), and NiO(L)/YSZ(S), respectively. That is, the cermets from $Ni(NO_3)_2$/YSZ(S) have the lowest threshold value for forming a connective Ni network due to the incorporation of smaller Ni particles. This is in good agreement with the microstructural observations (Fig. 1). Consequently, it is possible to use less amount of Ni in Ni/YSZ anodes by decreasing Ni particle size. This is beneficial to decrease both shrinkage difference and thermal expansion mismatch between Ni/YSZ cermet anode and YSZ electrolyte layers in SOFCs.

Fig. 3 shows the dependence of porosity in sintered and reduced samples on volume fraction of Ni. As the Ni content rose, the porosity increased

almost linearly. The composites from finer NiO(S) powder showed higher porosity than those from NiO(L) powder. With regard to the composites obtained from nickel nitrate, the porosity had the highest values. This is associated with the inhibiting effect of NiO particles on densification of YSZ matrix. As the average size of NiO particles decreases, the inhibiting contribution becomes large, thus resulting in the increase in porosity. After reduction, the porosity in Ni/YSZ cermets was further increased.

From the above results, the composites obtained from $Ni(NO_3)_2$/YSZ has higher porosity than those from NiO/YSZ, whether they are sintered or reduced samples. As a consequence, the utilization of nickel nitrate not only promotes the formation of fine Ni network and causes improvements in electrical conductivity, but also leads to increase in porosity in Ni/YSZ cermets.

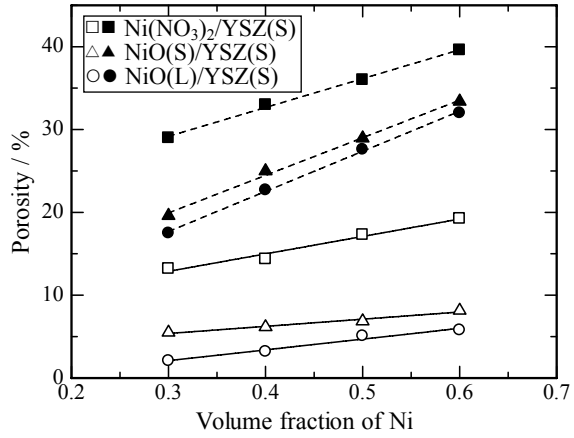


Fig. 3. Dependence of porosity on volume fraction of Ni. The solid and dotted lines represent the results of sintered and reduced samples, respectively.

### 3.2 Effect of YSZ Particle Size

As an example, Fig.4(a) shows the microstructure of a sintered NiO(L)/YSZ composite with a composition of $V_{Ni}$ = 0.3, where the YSZ consists of as-received fine YSZ(S) and pre-calcined coarse YSZ(L) powders (YSZ(S):YSZ(L)=2:1). It was seen from the micrograph that the pre-calcined powder included various particles with different sizes, indicating the presence of particle size distribution. The NiO phase with a gray contrast tends to be connected into a network. This microstructural feature is quite different from that shown in Fig. 1(a), where no pre-calcined YSZ(L) particles were involved and isolated NiO particles were distributed in YSZ matrix homogeneously. This indicates that the connection of NiO particles can be improved through incorporation of coarse YSZ particles. Furthermore, in those region without coarse YSZ(L) particles, from the image with a high magnification shown in Fig. 4(b), NiO and YSZ phases exhibited an interconnected and fine structure, in which YSZ phase is believed to result from the original fine YSZ(S) powder. This characteristic microstructure is thought to be effective to prevent Ni particles from agglomeration or coarsening during cell preparation and operations. With the increase in mixing ratio of coarse particles, the connection of NiO particles themselves was further improved.

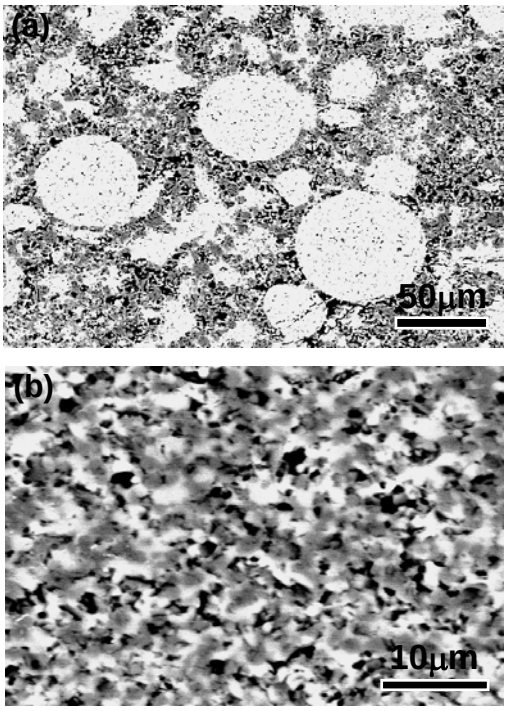


Fig. 4. Microstructures of NiO(L)/YSZ composites ($V_{Ni}$ =0.3), showing the effect of pre-calcined YSZ powder (YSZ(S):YSZ(L)=2:1).

The development of NiO network due to addition of pre-calcined particles can also be explained by the percolation theory. Relative to YSZ(S) and NiO(L) powders, YSZ(L) has a much larger average size (47.3μm). Hence, when YSZ(L) is incorporated into NiO(L)/YSZ(S) system, the ratio between matrix (YSZ) and second phase (NiO) becomes large, thus promoting the formation of NiO percolative network in YSZ matrix. On the contrary, because of a small particle size ratio (0.054) between

YSZ(S) (matrix) and NiO(L) (second phase), the NiO particles are distributed in the YSZ matrix randomly (Fig. 1(a)), although the content of NiO is the same ($V_{Ni}$ = 0.3) as that shown in Fig. 4(a).

Fig.5 shows the variation of electrical resistivity against volume fraction of Ni for Ni/YSZ cermets which were prepared from NiO(L)/YSZ(S)/ YSZ(L) powder mixtures. In comparison with the cermets without addition of pre-calcined YSZ powder (YSZ(S):YSZ(L)=1:0), the cermets containing fine and coarse YSZ powders had lower values of electrical resistivity. As the mixing ratio of coarse particles increased, the value of electrical resistivity was lower. These results are consistent with the configurational change of Ni phase and development of Ni network in the cermets.

The addition of pre-calcined YSZ powder can also cause change in porosity. The dependence of porosity in sintered and reduced samples with and without addition of pre-calcined powder on volume fraction of Ni is shown in Fig. 6. The incorporation of coarse YSZ particles led to improvement in porosity for both sintered and reduced composites. As the amount of pre-calcined particles increased, a higher level of porosity was achieved. The increase in porosity may be attributed to the following two reasons: (a) small driving force for sintering due to a large average particle size of YSZ(L) powder and (b) inhibiting effect of YSZ(L) particles on densification of both NiO(L) and YSZ(S) powders during sintering.

To examine the effect of pre-calcined coarse YSZ(L) powder on densification behavior of NiO(L)/YSZ(S)/YSZ(L) powder mixtures, the relationship between linear shrinkage and heating time or temperature during sintering has been measured by TMA, and the results are shown in Fig. 7. For the purpose of comparison, the shrinkage behavior of YSZ electrolyte ($V_{Ni}$ = 0) is also shown in the figure. For all specimens with different compositions, sintering shrinkage starts to occur at ~1300K. Above 1300K, the shrinkage increases rapidly, but the densification rate depends on powder composition and mixing ratio of the coarse powder. It can be found from Fig.7 that the majority of sintering shrinkage occur in the latter stage of heating close to the temperature of isothermal sintering (1673K) and during the isothermal sintering. The YSZ electrolyte prepared from YSZ(S) powder only exhibited the largest amount of shrinkage. This is due to its smaller average particle

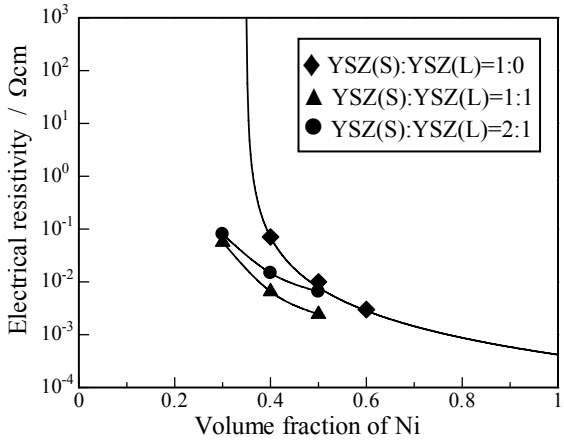


Fig. 5. Variation of electrical resistivity against $V_{Ni}$ for Ni/YSZ cermets containing pre-calcined YSZ powder with different mixing ratios.

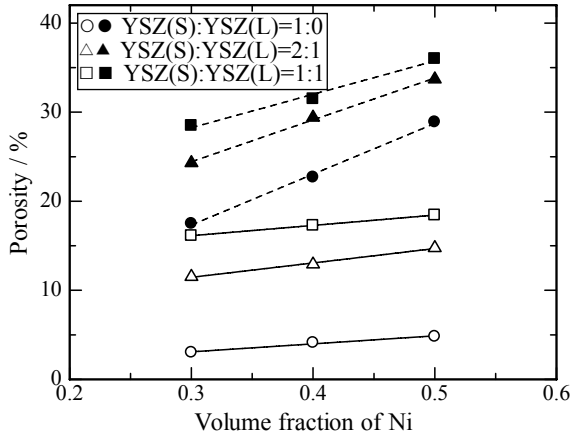


Fig. 6. Dependence of porosity on volume fraction of Ni, reflecting the effect of pre-calcined coarse YSZ particles. The solid and dotted lines represent the results of sintered and reduced samples, respectively.

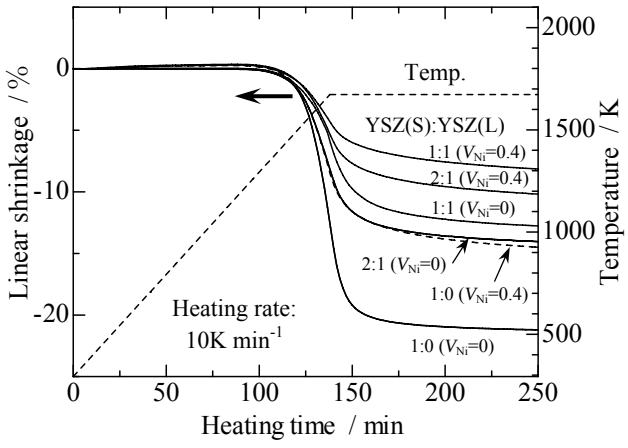


Fig. 7. Relationship between linear shrinkage and heating time or temperature, measured by thermomechanical analysis.

size (0.54μm) and larger specific surface area, *i.e.*, larger driving potential for densification, as compared to YSZ(L) (47.3μm) and NiO(L) powders (4.7μm). When YSZ(S)/YSZ(L) powder mixtures are sintered, the shrinkage becomes smaller. Furthermore, the magnitude of shrinkage is dependent on the mixing ratio of the coarse powder. A larger mixing ratio leads to lower shrinkage. On the other hand, when NiO powder is added to YSZ matrix, the value of shrinkage decreases as well, because of the inhibiting effect of NiO particles on sintering densification.

On the basis of the results described above, the incorporation of pre-calcined YSZ powder in Ni/YSZ anodes results in development of Ni network, improvement in electrical conductivity, and increase in porosity. At the same time, however, the linear shrinkage during sintering is reduced. This may cause some problems in sintering shrinkage difference and CTE mismatch between Ni/YSZ anode and YSZ electrolyte. On the other hand, for YSZ electrolyte, as shown in Fig. 7, YSZ(S) and YSZ(L) powder mixtures showed lower values of shrinkage. Accordingly, it might be possible to decrease the difference in sintering shrinkage by (a) decreasing Ni content in Ni/YSZ anode and (b) introducing certain amount of pre-calcined coarse YSZ powder into YSZ electrolyte.

## 4 Conclusions

The effect of particle sizes of two constituent components (Ni and YSZ) on microstructure (especially development of Ni network), electrical conductivity, and porosity of Ni/YSZ cermets has been investigated. Ni particles with submicron order can be incorporated into YSZ matrix by using nickel nitrate as one of the starting materials, which is decomposed and then reduced into metallic Ni. The formation of small-sized Ni particles promotes the development of a continuous Ni network and results in improvements in electrical conductivity and porosity. Accordingly, it is possible to use less amount of Ni in Ni/YSZ anodes by decreasing Ni particle size, which is beneficial to decrease shrinkage difference and thermal expansion mismatch between Ni/YSZ cermet anode and YSZ electrolyte layers in SOFCs.

On the other hand, the incorporation of coarse YSZ particles, obtained by calcining commercial fine YSZ powder at high temperature, is effective in forming a continuous Ni network in Ni/YSZ cermets. Furthermore, the electrical conductivity and porosity can also be improved, but coarse YSZ powder causes decrease in linear shrinkage.

## References


[1] Badwal S.P.S. and Foger K. “Materials for solid oxide fuel cells”. *Mater. Forum,* Vol. 21, pp 187-224, 1997.

[2] Clemmer R.M.C. and Corbin S.F. “Influence of porous composite microstructure on the processing and properties of solid oxide duel cell anodes”. *Solid State Ionics*, Vol. 166, pp 251-259, 2004.

[3] Setoguchi T., Okamoto K., Eguchi K. and Arai H. “Effects of anode material and fuel on anodic reaction of solid oxide fuel cells”. *J. Electrochem. Soc*., Vol. 139, No. 10, pp 2875-2880, 1992.

[4] Minh N.Q. “Ceramic fuel cells”. *J. Am. Ceram. Soc*., Vol. 76, No. 3, pp 563-588, 1993.

[5] Itoh H., Yamamoto T., Mori M., Horita T., Sakai N., Yokokawa H. and Dokiya M. “Configurational and electrical behavior of Ni-YSZ cermet with novel microstructure for solid oxide fuel cell anodes”. *J. Elctrochem Soc*., Vol. 144, No. 2, pp 641-646, 1997.

[6] Chen Z., Takeda T., Kikuchi K., Kikuchi S. and Ikeda K. “Preparation of anode/electrolyte ceramic composites by coextrusion of pastes”. *J. Am. Ceram. Soc*., Vol. 87, No. 6, pp 983-990, 2004.

[7] Jia L., Lu Z., Miao J., Liu Z., Li G. and Su W. “Effects of pre-calcined YSZ powders at different temperatures on Ni-YSZ anodes for SOFC”. *J. Alloys Comp*., Vol. 414, pp 152-157, 2006.

[8] Wang Y., Walter M.E., Sabolsky K. and Seabaugh M.M. “Effects of powder sizes and reduction parameters on the strength of Ni-YSZ anodes”. *Solid State Ionics*, Vol. 177, pp 1517-1527, 2006.

[9] Kawada T., Sakai N., Yokokawa H., Dokiya M., Mori M. and Iwata T. “Structure and polarization characteristics of solid oxide fuel cell anodes”. *Solid State Ionics*, Vol. 40-41, No. 1, pp 402-406, 1990.

[10] Zallen R. “*The physics of amorphous solids*”. Wiley, New York, 1983.

[11] Malliaris A. and Turner D.T. “Influence of particle size on the electrical resistivity of compacted mixtures of polymeric and metallic powders,” *J. Appl. Phys*., Vol. 42, No. 2, pp 614-618, 1971.

[12] Kusy R.P. “Influence of particle size ratio on the continuity of aggregates”. *J. Appl. Phys*., Vol. 48, No. 12, pp 5301-5305, 1977.

[13] Bouvard D. and Lange F.F. “Relation between percolation and particle coordination in binary powder mixtures,” *Acta Metall. Mater*., Vol. 39, No. 12, pp 3083-3090, 1991.

[14] Chen Z., Takeda T., Ikeda K. and Murakami T. “The influence of powder particle size on microstructural evolution of metal-ceramic composites”. *Scr. Mater.*, Vol. 43, No. 12, pp 1103-1109, 2000.